



HAL
open science

High tunability in lead-free Ba_{0.85}Sr_{0.15}TiO₃ thick films for microwave tunable applications

Selmi Aymen, Manuel Mascot, Fathi Jomni, Jean-Claude Carru

► To cite this version:

Selmi Aymen, Manuel Mascot, Fathi Jomni, Jean-Claude Carru. High tunability in lead-free Ba_{0.85}Sr_{0.15}TiO₃ thick films for microwave tunable applications. *Ceramics International*, 2019, 45 (17), pp.23084-23088. <10.1016/j.ceramint.2019.07.357>. <hal-03488694>

HAL Id: hal-03488694

<https://hal.science/hal-03488694v1>

Submitted on 20 Jul 2022

HAL is a multi-disciplinary open access archive for the deposit and dissemination of scientific research documents, whether they are published or not. The documents may come from teaching and research institutions in France or abroad, or from public or private research centers.

L'archive ouverte pluridisciplinaire HAL, est destinée au dépôt et à la diffusion de documents scientifiques de niveau recherche, publiés ou non, émanant des établissements d'enseignement et de recherche français ou étrangers, des laboratoires publics ou privés.



Distributed under a Creative Commons CC BY-NC 4.0 - Attribution - Non-commercial use - International License

High tunability inlead-free $\text{Ba}_{0.85}\text{Sr}_{0.15}\text{TiO}_3$ thick films for microwave tunable applications

Aymen Selmi^{a, b*}, Manuel Mascot^b, Fathi Jomni^a, Jean-Claude Carru^b

^a*Université de Tunis El Manar, Laboratoire Matériaux Organisation et Propriétés (LR99ES17), 2092 Tunis, Tunisia*

^b*Université du Littoral-Côte d'Opale, Unité de Dynamique et Structure des Matériaux Moléculaires (UDSMM), 62228, Calais, France*

*Corresponding author: E-mail address: eyman_selmi@yahoo.fr, Phone: (+216) 21 061 882

Abstract

Lead free ferroelectric **Ba_{0.85}Sr_{0.15}TiO₃(BST)** thick films were successfully deposited by screen printing process on Ag-Pd/Al₂O₃ substrates. The microstructure of the samples was analyzed by scanning electron microscope (SEM) and X-ray diffraction (XRD). **The thick films** showed a good adhesion to the Ag-Pd/Al₂O₃ substrate, a porous microstructure and uniform **thicknesses** of about 10 μm. The dielectric **properties** of BST thick films were studied over a wide frequency range (10⁻¹ Hz to 10⁶ Hz) and **in a large temperature range from 25 °C to 350 °C**. The AC conductivity in **BST** thick films was systematically investigated. Ferroelectric characterizations and tunability were also studied at room temperature by polarization cycles P(E) and **capacitance C(E)** measurements. The high values of dielectric permittivity and tunability (67%) combined with low dielectric loss (tgδ) make Ba_{0.85}Sr_{0.15}TiO₃ thick films one of the encouraging candidates for microwave tunable applications.

Keywords: **Barium strontium titanate; Thick films;** Screen printing; Dielectric properties; ac conductivity; Tunability.

1. Introduction

Ferroelectric oxide materials have been studied for a long time, but only recently have they been deposited in the form of thin and thick films with a thickness lower than $1\mu\text{m}$ and $500\mu\text{m}$ respectively. The electrical characteristics of ferroelectric materials are currently used to realize electronic components [1-3]. Their principal properties are large dielectric permittivity, high tunability, low microwave losses and non-linear polarization. Lead zirconate titanate (PbZrTiO_3 or PZT) is the most important ferroelectric material used in microelectronics. In fact, it has many applications such as pyroelectric infrared detectors, ferroelectric memories, capacitors, tunable microwave components, filters, etc... However, its main drawback is to contain lead which is strictly forbidden since July 2014 by the European directive RoHS. This directive bans the use of several polluting materials in electronic and microelectronic devices, including lead. Nevertheless, lead oxide based ferroelectric materials are yet used for their unique properties but in the near future they will be prohibited. The search to discover an alternative to PZT has started in many laboratories but it mainly concerns the ceramic form. Consequently, there is an urgent need to find alternative materials to PZT. Our research is focused on lead-free $\text{Ba}_{0.85}\text{Sr}_{0.15}\text{TiO}_3$ (BST), a good candidate to replace PZT in several uses [4]. This composition (BST85/15) is a good trade-off to have very good ferroelectric and dielectric properties for applications at temperatures close to room temperature. So, $\text{Ba}_x\text{Sr}_{1-x}\text{TiO}_3$ is the most extensively investigated material to date thanks to the high dielectric permittivity, small dielectric losses, low leakage-current density and other excellent physical properties. For applications in electronic devices, $\text{Ba}_x\text{Sr}_{1-x}\text{TiO}_3$ has been investigated in varied material forms, including thin films ($t < 1\mu\text{m}$), thick films ($1\mu\text{m} < t < 500\mu\text{m}$) and ceramics ($t > 500\mu\text{m}$) [5,6]. At present, the majority of the works on ferroelectric oxides is oriented towards the form of thin films and/or ceramics. So far, BST thick films have been less reported. Yet BST thick films present a potential benefit of lower fabrication cost in comparison with that of thin film forms and low bias voltages required for tunability in relation to the thickness of ceramics. BST thick films also strongly fill the technological difference between thin films and ceramics. Several techniques have been successfully used to elaborate BST thick films including sol-gel, pulsed laser deposition, and screen printing [7-9]. Among these different processes, screen printing is a viable, low-cost and practical procedure for wide area elaboration of thick films. This technique is suitable for coating surfaces of whatever geometry and morphology and has been applied to produce several ferroelectric thick films such as PZT [10], BZN [11] and BST [9].

In this study, Ba_{0.85}Sr_{0.15}TiO₃ thick films were successfully deposited by screen printing on alumina substrates covered with a silver-palladium electrode. The dielectric **properties** of Ba_{0.85}Sr_{0.15}TiO₃ thick films were studied as a function of temperature and frequency. Various AC electrical **measurements** such as dielectric permittivity, dielectric loss tangent ($\tan\delta$) and AC conductivity **were made** in order to better **understand** the correlation between the microstructure of the thick films and the dielectric response. Ferroelectric properties of BST thick film have also been analyzed using Capacitance-Electric field (C-E) and Polarization-Electric field (P-E) measurements. It is shown that **our** BST thick films present high tunability (67%) and good dielectric properties **which** compare **well with BST both** in thin films and **in** ceramics.

2. Experimental

2.1 Thick film preparation

Ba_{0.85}Sr_{0.15}TiO₃ thick films were elaborated by using a screen-printing device (TIFLEX - HL570S). BST powders were synthesized by the solid-state procedure from strontium oxide (SrO), barium oxide (BaO) and titanium oxide (TiO₂). The ink for screen printing **was prepared by mixing BST** powders with organic vehicles. The organic vehicles were composed of {alpha-terpineol (C₁₀H₁₈O), polyvinyl butyral (C₈H₁₄O₂)_n, 2-(2-butoxyethoxy)-ethyl acetate (C₁₀H₂₀O₄) and polyethylene glycol (C₂H₄O)} **from ARCOS ORGANICS**. The ink was mixed and milled by a roller to obtain a perfect uniform homogeneity. Initially polyvinyl butyral **was** dissolved in α -terpineol at 60 °C with vigorous stirring for 30 minutes. The Ba_{0.85}Sr_{0.15}TiO₃ powder (previously dissolved in 2-(2-Butoxyethoxy) ethyl acetate) was added and the polyethylene glycol was added to stabilize the mixture. After 1 hour, the ink was heated at 100 °C for 1 hour to evaporate the solvent. Finally, the ink passes to ultrasound and between the three-cylinder roller in order to break the agglomerates. **High** purity alumina substrates were covered by a silver-palladium **paste** to **realize** the **bottom** electrode for the electrical characterizations. The Ag-Pd paste was deposited via **spin-coater** on alumina substrates and heated at 1100 °C for 1 h. The ink was deposited by screen printing on the Ag-Pd and **heated** at 100 °C for 1 h. This **procedure** was repeated two times. Thereafter, the BST thick films were sintered in air for 2 h at 1100 °C. Finally, gold circular electrodes (**top** electrodes) with different diameters, **from** 0.1 mm **to** 2 mm **were** evaporated through a shadow mask on the BST thick films to obtain MIM (**metal-**

insulator-metal) structures for the electrical measurements. The different main steps of preparation are shown in Fig. 1.

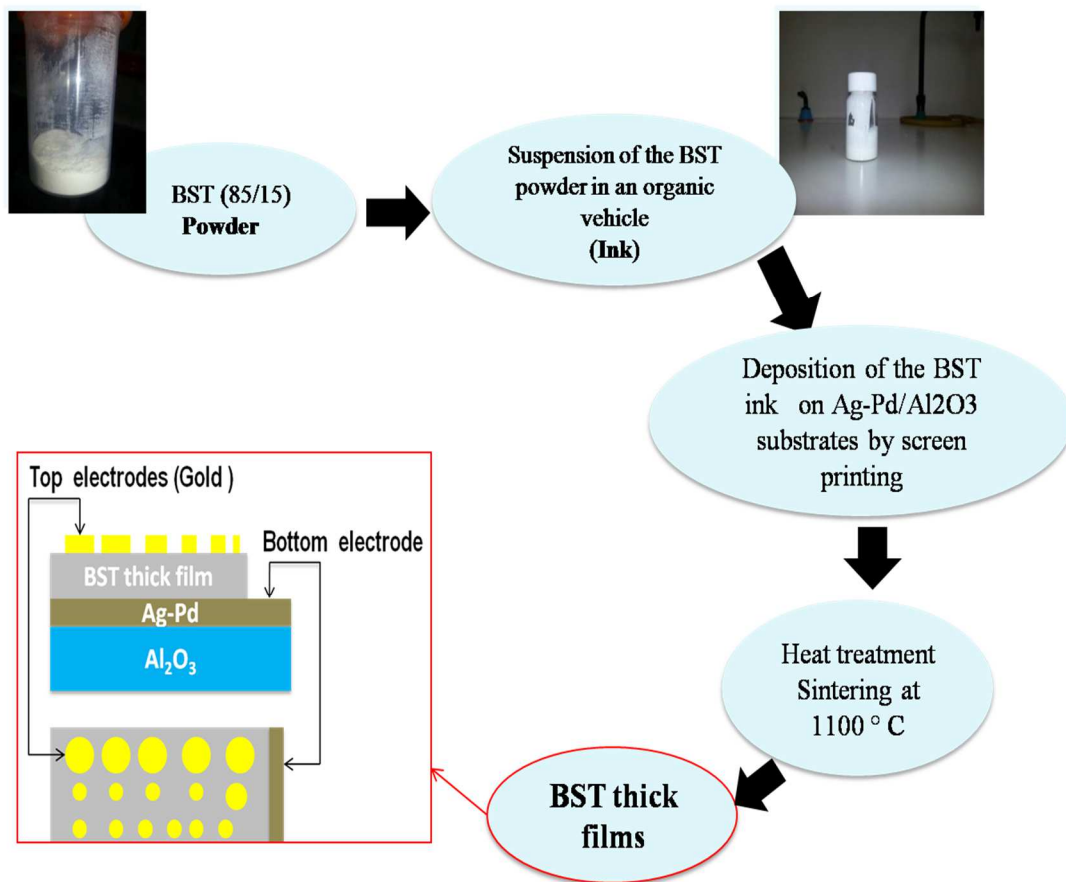


Figure 1.

2.2 Characterizations techniques

The crystallographic microstructure and the morphology of the samples were characterized by X-Ray Diffraction **with a Philips diffractometer (model PW1710)** and Scanning Electron Microscopy (**JEOL JSM-5400**). The electrical properties of BST were measured over a large frequency range (10^{-1} to 10^6 Hz) in the 25°C-350°C **temperature** range using a Solartron 1260A **Impedance Analyzer with a Dielectric Interface 1296**. Capacitance-Voltage (C-E) measurements of the Au/BST/Ag-Pd capacitor **were** performed using an Agilent LCR meter E4980A. **The hysteresis cycles were recorded with a modified Sawyer Tower circuit at a frequency of 1 kHz.**

3. Results and discussion

3.1 Structural and morphological investigation

Fig. 2 shows the XRD diffractogram of the BST thick film. It can be observed from the graph the existence of diffraction peaks indexed to (100), (110), (111), (200), (210) and (211) planes. They are characteristic of BST (JCPDS File no. 39-1395) in the (10°-60°) 2θ range. In addition, the calculated a-axis and c-axis lattice values are 3.9942 Å and 4.0171 Å respectively. This suggests that the film is crystallized with the tetragonal structural phase. Small alumina and silver phases were also detected, which are associated with the substrate and the bottom electrode respectively.

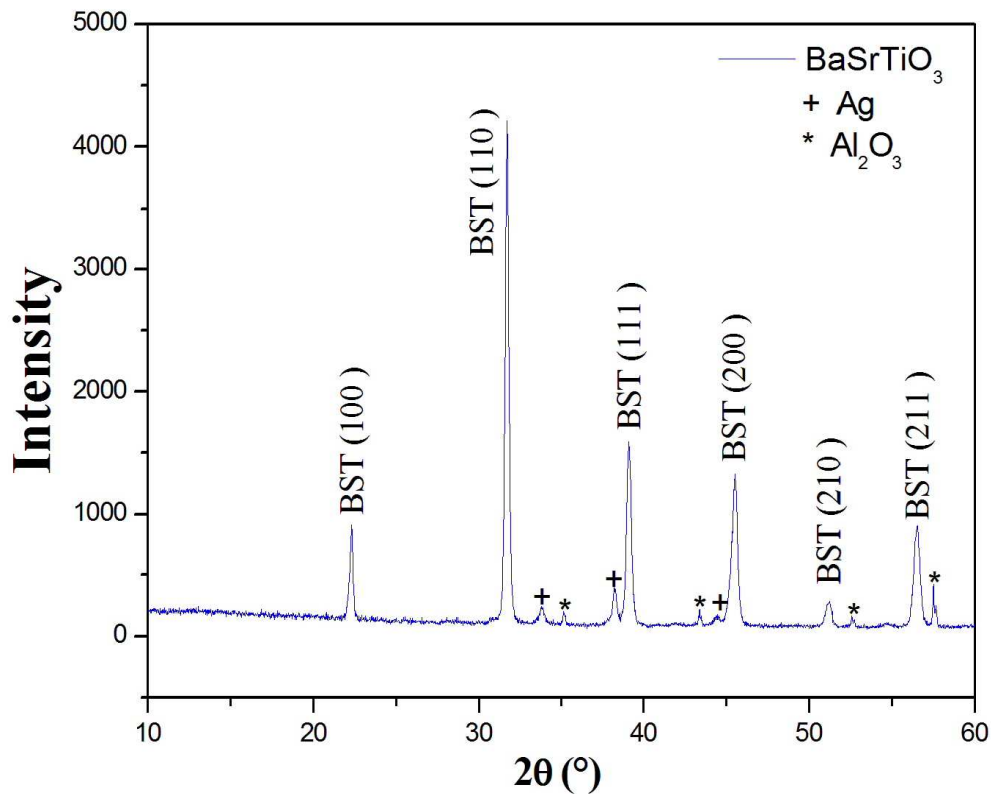


Figure 2.

Fig. 3 exhibits the SEM images of the BST thick film. Figs. 3a and 3b show the cross-section view and a portrait zoom on the BST layer, respectively. It is clear that no cracks on the BST film were observed. The image zoom on BST presents a porous microstructure and the

average grain size is $0.4\ \mu\text{m}$. The cross-section view shows a generally uniform thickness of about $9\ \mu\text{m}$ and an excellent adhesion to the Ag-Pd/ Al_2O_3 substrate.

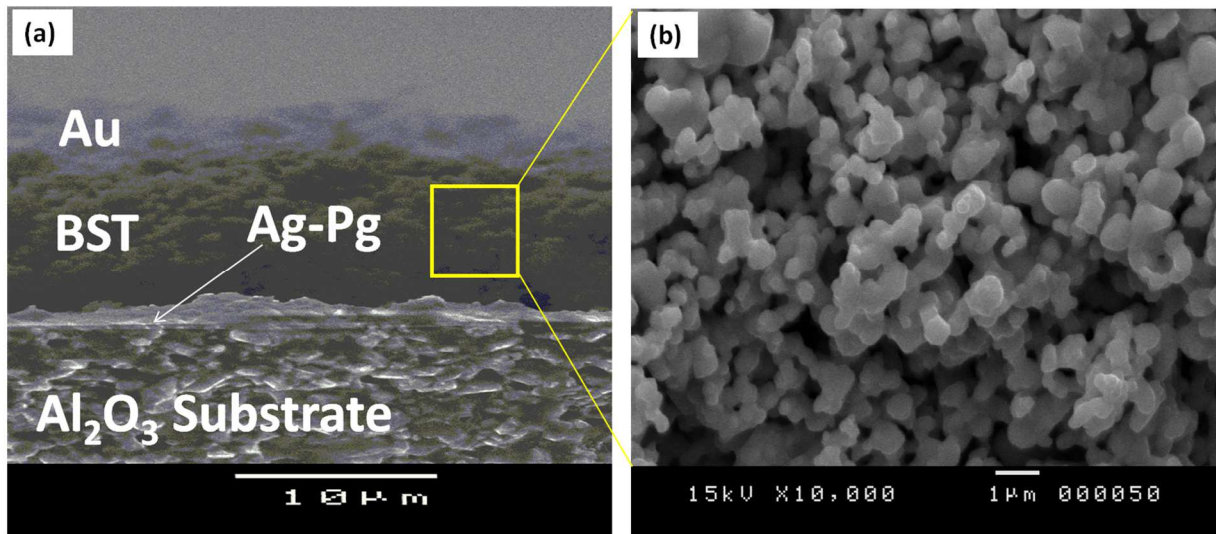


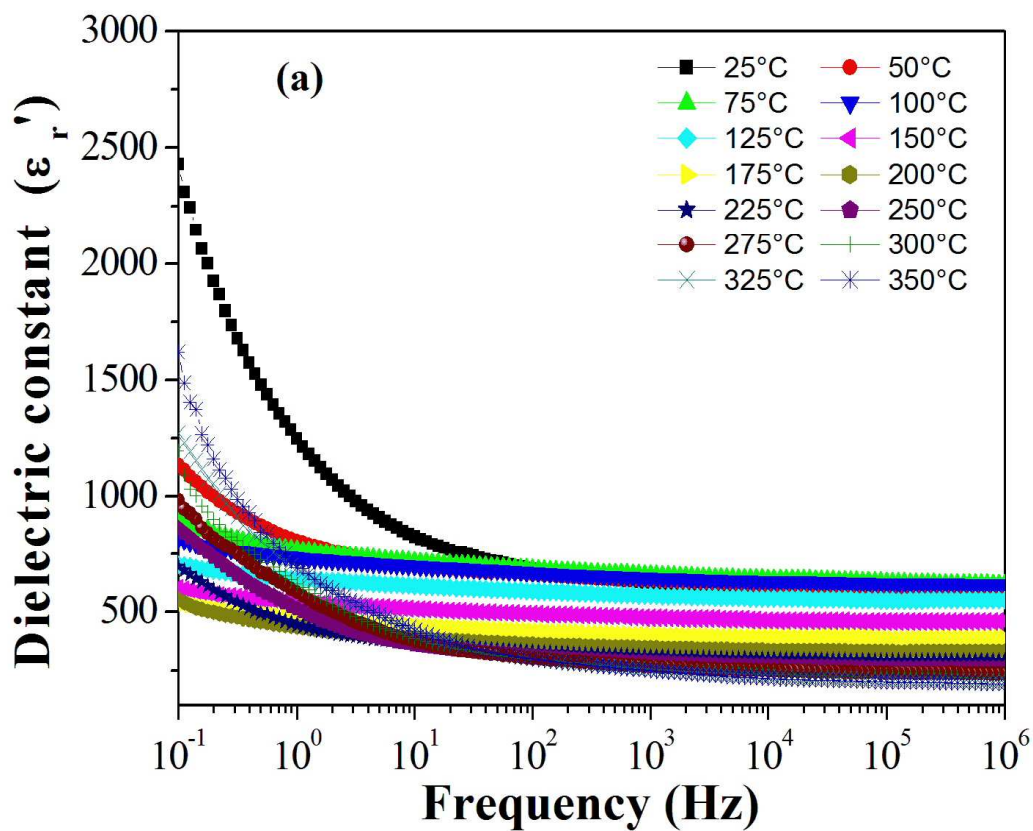
Figure 3.

3.2 Dielectric Analysis

3.2.1. Permittivity and loss studies

Dielectric properties of BST thick film were studied **as a function of** frequencies (0.1 Hz to 1 MHz) and **in the** temperature range 25°C - 350°C . The evolution of **the** dielectric **permittivity** ϵ'_r from the complex permittivity $\epsilon^* = \epsilon'_r - i\epsilon''_r$ [12] of **the BST film** is shown in Fig. 4.a. **It is clear that for all temperature the dielectric permittivity decreases rapidly in the low-frequency region and then go more or less stable at higher frequencies. The high value of the dielectric permittivity and the dispersion behavior at lower frequencies can be explained by the dominance of grain boundaries effect. This is an extrinsic contribution associated to the Maxwell-Wagner interfacial polarization in agreement with Koops phenomenological theory [13]. According to this theory, a dielectric oxide material is made up of conducting grains segregated by highly resistive grain boundaries. The grain boundaries are more effective at low frequencies while the grains are found to be more effective in the high frequencies. Under the effect of the applied electric field, there is an accumulation of electric charge at the interfaces of the grains and the grain boundaries (interfacial polarization). After the initial great value at low frequencies, ϵ'_r becomes nearly constant at frequencies higher than 100Hz. This is due to**

an intrinsic contribution of the ferroelectric domains in the grains of the BST film. It is important to note that the dielectric permittivity shows a comparable value, **above 100 Hz**, to **data** found on BST ceramic [14] and **also** presents an excellent stability in a large frequency range. This result is heartening for microwaves applications. **The dielectric loss tangent ($\text{tg}\delta = \epsilon''/\epsilon'$) has also been measured at different temperatures.** The curves obtained for **$\text{tg}\delta$** are presented in Fig.4b. These **curves** show the same behavior **that** of the dielectric permittivity: for each temperature the dielectric losses **decrease when the frequency increases** due to Maxwell-Wagner interfacial polarization [7].



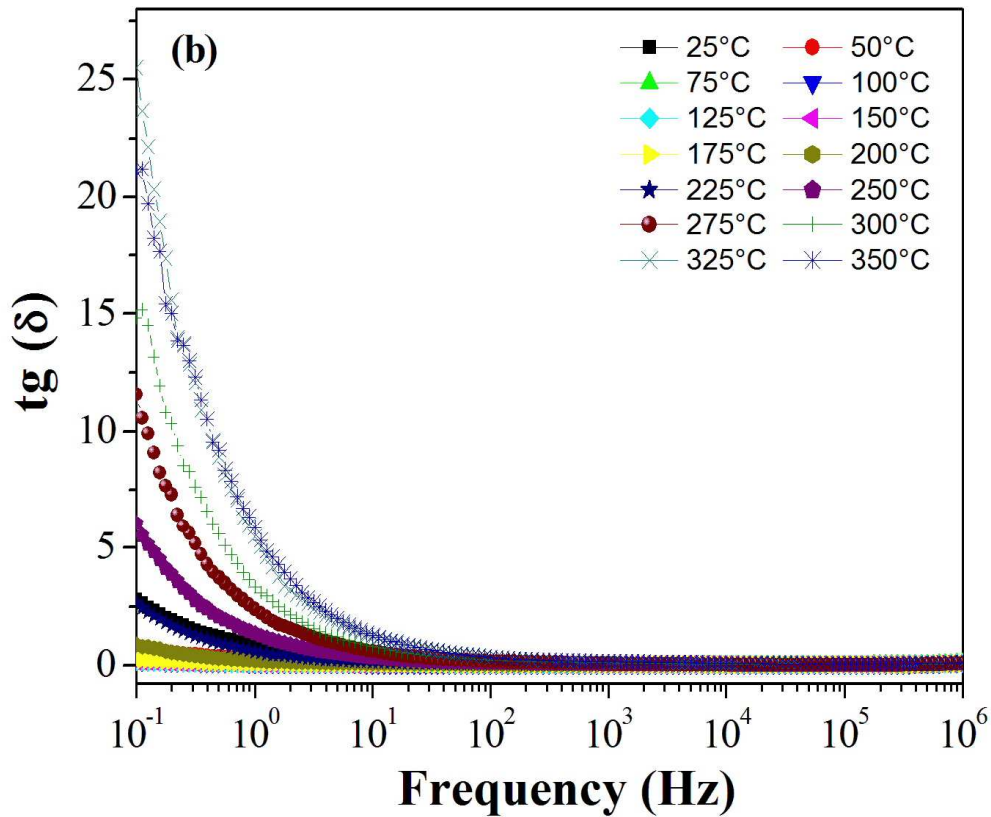
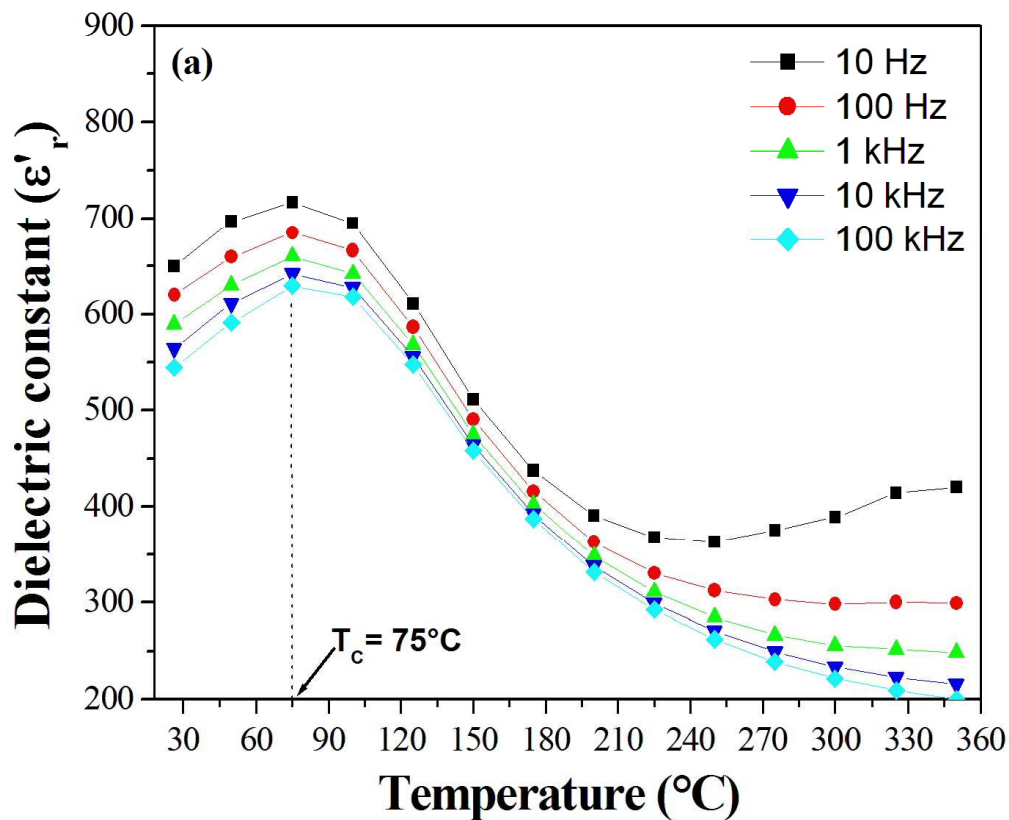


Figure 4.

The variation of ϵ'_r and $\tan\delta$ of BST thick film with temperature for several frequencies is represented in Fig. 5. For all frequency values, the dielectric permittivity shows, in Fig. 5a, a large peak at a Curie temperature $T_C = +75^\circ\text{C}$. This observed peak corresponds to a ferroelectric–paraelectric phase transition in the BST system. From 25°C to 75°C it is admitted that the increase of ϵ'_r characterizes the ferroelectric state while above 75°C the monotonous decrease of ϵ'_r characterizes the paraelectric state where the ferroelectric domains progressively disappeared when the temperature increases. Moreover, the value of T_C is smaller than the one found on a BST in the ceramics form [14] where $T_C = +101^\circ\text{C}$. This variance is possibly associated to the small grain size in a thick film compared with a ceramic and may also be related to a little difference of composition as the T_C is very sensitive to the Ba/Sr ratio which is here 90/10 for the ceramic. For instance, our value of $T_C = +75^\circ\text{C}$ is for a 85/15 ratio while $T_C = -2^\circ\text{C}$ for a 60/40 ratio on a BST thick film also deposited by screen printing [6]. The value of T_C found on our thick films confirms that the BST is in ferroelectric phase at room temperature. This result is encouraging for several

applications including high dielectric constant capacitors, super-capacitors and ferroelectric random-access memories (FRAM). The thermal evolution of the dielectric loss tangent for different frequencies (Fig. 5b) gives low values ($\tan\delta < 0.1$) in large temperature, ranging from 25 °C to 150°C. Above 150 °C the dielectric losses show an important increase which can be attributed to the motion of oxygen vacancies. In fact, oxygen vacancies are thermally activated and then can make hopping in the grains and grains boundaries which increase the losses [15]. The high values of the dielectric permittivity and the associated low losses values obtained over a wide temperature range (25-150 °C) make the $\text{Ba}_{0.85}\text{Sr}_{0.15}\text{TiO}_3$ thick films one of the possible candidates for the different applications mentioned above.



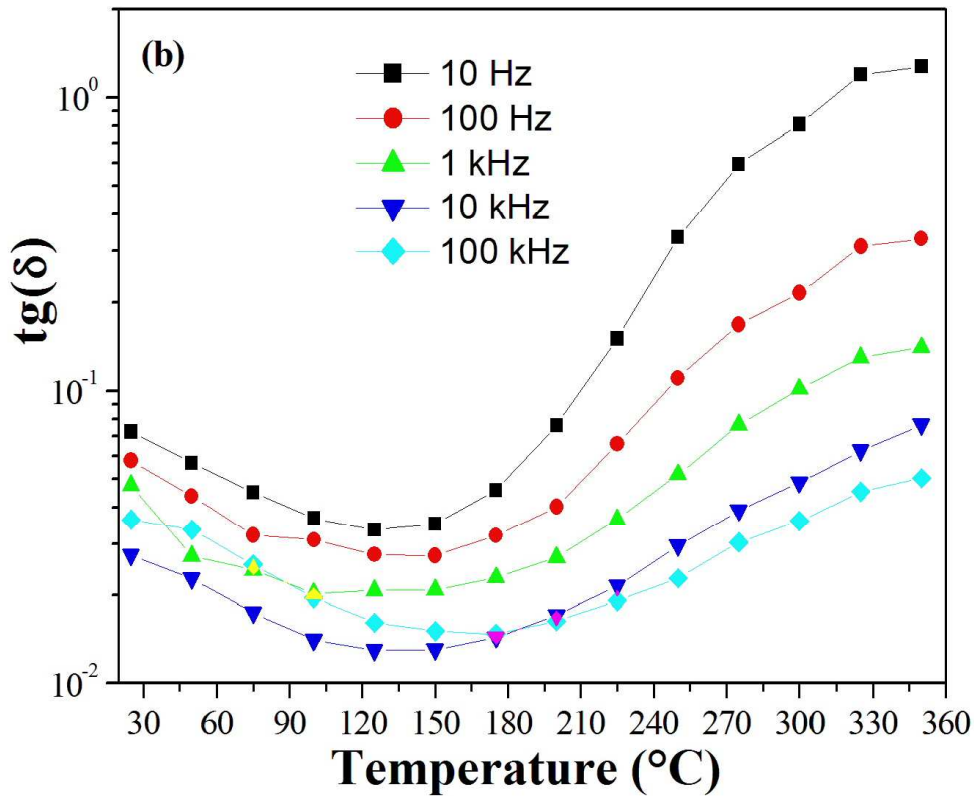


Figure 5.

3.2.2.AC Conductivity Analysis

The AC conductivity (σ_{ac}) of the BST thick film was obtained from the determination of ϵ'_r and $\tan\delta$ and calculated with the following formula [16]:

$$\sigma_{ac} = \omega \epsilon'_r \epsilon_0 \tan(\delta) \quad (1)$$

Where ϵ_0 is the vacuum permittivity and $\omega = 2\pi f$ is the angular frequency.

Frequency dependent AC conductivity was measured in the frequency range $0.1 \text{ Hz} \leq F \leq 10^6 \text{ Hz}$ at various temperatures (225°C-350°C) and is shown in Fig. 6. In the low frequency region, for all temperatures, the conductivity is practically independent of frequency [17], this is associated with the DC conductivity (σ_{dc}) of the BST. Above about 1 Hz and up to 1 MHz, the AC conductivity increases strongly, for example of 4 decades at 300 °C. The AC conductivity of BST can be interpreted by the Jonscher's law of the Universal Dielectric Response (UDR) model [18]:

$$\sigma_{ac} = \sigma_{dc} + A\omega^n \quad (2)$$

Fig.6 presents the theoretical fits of the experimental data of σ_{ac} with equation (2). From this figure, it can be seen that the experimental data are well fitted with the UDR model. In order to specify the principal conduction mechanism of the AC conductivity, the variation of 'n' with temperature reveals that the exponent 'n' decreases when the temperature increases (not shown here). This trend shows that the AC conduction in BST thick film follows the Correlated Barrier Hopping (CBH) model [19]. Also, from Fig. 6 and the σ_{dc} values obtained with the fit, it's clear that the stationary regime is thermally activated so the conductivity σ_{dc} can be represented by the Arrhenius law [16]:

$$\sigma_{dc} = \sigma_0 e^{\left[\frac{-E_\sigma}{k_B T}\right]} \quad (3)$$

where T is the temperature in Kelvin, k_B is the Boltzmann constant, σ_0 is the pre-exponential factor and E_σ is the DC conductivity activation energy. The extracted activation energy value for DC conduction was found to be around 0.5 eV. According to the literature, this value is comparable to the energy required for a polaron to jump [14,20,21] through the grain boundaries. **These polarons can be constituted by electrons associated with singly and doubly positively charged oxygen vacancies O_o^\bullet and $O_o^{\bullet\bullet}$ (with Kroger-Vink notation). As stated in the previous paragraph, these jumps are at the origin of the dielectric losses observed above 150 °C in the measurement frequency range. So, it can be concluded that at high temperature, typically above 150 °C, the DC conductivity and the dielectric loss $\tan \delta$ have the same origin that is to say the hopping of polarons.**

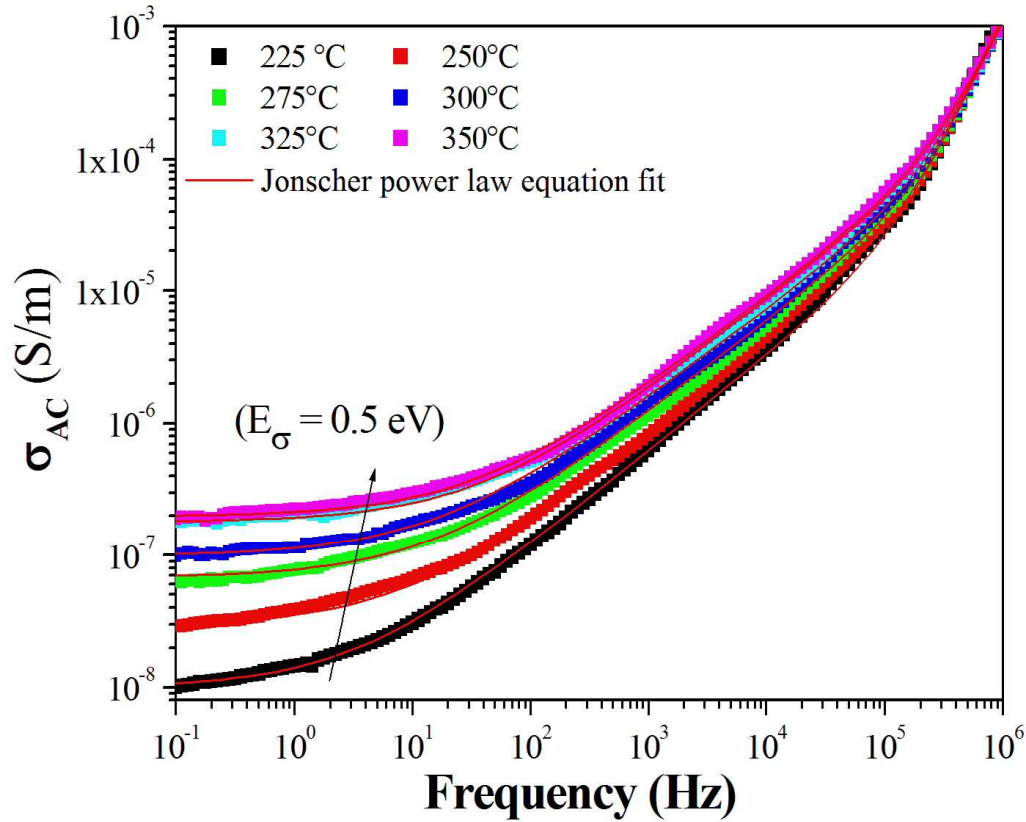


Figure 6.

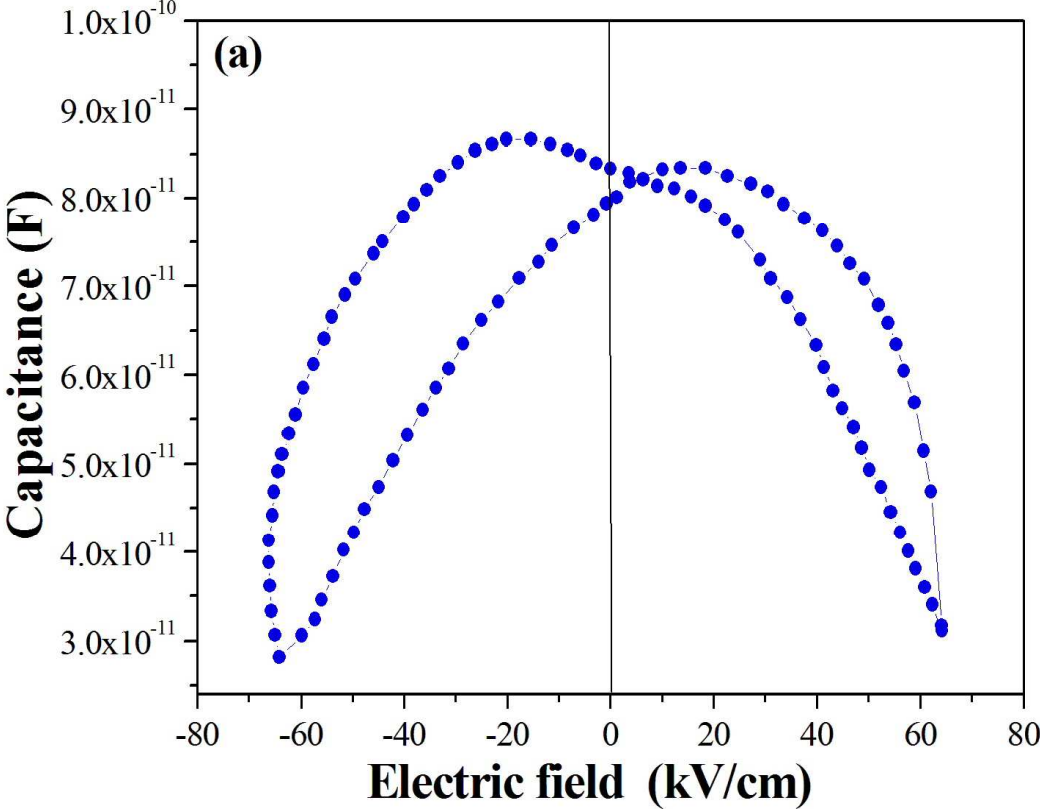
3.3. Capacitance-electric field (C-E) and polarization-electric field (P-E) measurements

Fig. 7a shows the capacitance- electric field response at room temperature for a BST thick film. The butterfly form of the curve confirms the ferroelectric behavior of the film. The dielectric tunability was obtained using the following formula [22]:

$$\frac{C(0) - C(E)}{C(0)} * 100 \quad (4)$$

where $C(0)$ is the capacitance at 0 kV/cm and $C(E)$ is the capacitance for an electric field of value E . The tunability at 12Volts and at 1kHz is about 67%:this value is higher than those recently published with BST thin films[4, 23, 24] and comparable to that published on BST ceramics[25].This value highlight that the high tunability of our BST thick films is very encouraging formicroelectronic applications such as tunable capacitors in radiofrequencies. The hysteresis cycle of the Au/BST(thick film)/Ag-Pd structure was recorded at room temperature at 1 kHz (Fig. 7b). The existence of a hysteresis loop confirms that the sample is ferroelectric in nature. From the hysteresis loop, the remanent polarization

value is estimated to be $0.92\mu\text{C}/\text{cm}^2$, the maximum polarization is $3.5\mu\text{C}/\text{cm}^2$ and the coercive field is about $6\text{ kV}/\text{cm}$ at room temperature.



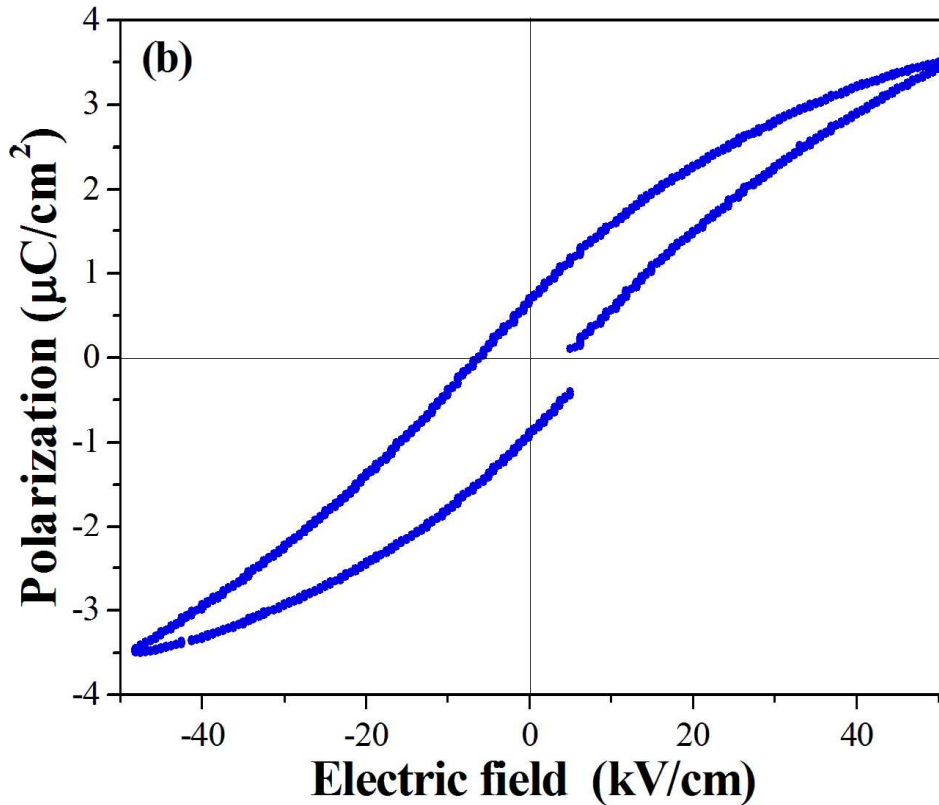


Figure 7.

4. Conclusions

We have shown that it is feasible to elaborate by a low-cost technique, namely a conventional screen-printing method, good quality lead free $\text{Ba}_{0.85}\text{Sr}_{0.15}\text{TiO}_3$ films **of at least 10 μm thick.** **The electrical characteristics of our BST films** are comparable and sometimes better than the ones of BST thin films and ceramics. This material is very **interesting** in the area of thick film technology and presents an alternative **to Pb-based ferroelectric materials.** The high values of dielectric permittivity and tunability (67%) combined with low dielectric loss **tangent** make $\text{Ba}_{0.85}\text{Sr}_{0.15}\text{TiO}_3$ thick films **usable** for functional applications like tunable ferroelectric capacitors **in radiofrequencies and in microwaves.**

Acknowledgments

The authors thank Didier Fasquelle and Mohamad Ali El Romeh for their help in preparing the thick films.

References:

- [1] N. Setter, D. Damjanovic, L. Eng, G. Fox, S. Gevorgian, S. Hong, A. Kingon, H. Kohlstedt, N.Y. Park, G.B. Stephenson, I. Stolitchnov, A.K. Taganstev, D.V. Taylor, T. Yamada, S. Streiffer, Ferroelectric thin films: Review of materials, properties, and applications, *J. Appl. Phys.* 100, 051606 (2006).
- [2] S. Yu, L. Li, H. Zheng, Z. Sun, W. Zhang, $\text{Ba}_{0.6}\text{Sr}_{0.4}\text{TiO}_3\text{-Bi}_{1.5}\text{Mg}_{1.0}\text{Nb}_{1.5}\text{O}_7$ composite thin film capacitors with enhanced tunable performance for tunable device applications, *Materials Letters* 161 (2015) 517-519.
- [3] K. Froehlich, TiO_2 -based structures for nanoscale memory applications, *Materials Science in Semiconductor Processing* 16 (2013) 1186-1195.
- [4] D. Fasquelle, M. Mascot, N. Sama, D. Remiens, J.-C. Carru, Lead-free piezoelectric thin films for RoHS devices, *Sensors and Actuators A* 229 (2015) 30-35.
- [5] M. Mascot, D. Fasquelle, G. Velu, A. Ferri, R. Desfeux, L. Courcot, J.-C. Carru, Pyro, Ferro and Dielectric Properties of $\text{Ba}_{0.8}\text{Sr}_{0.2}\text{TiO}_3$ Films Deposited by Sol-Gel on Platinized Silicon Substrates, *Ferroelectrics* 362 (2008) 79-86.
- [6] X-F. Zhang, Q. Xu, D. Zhan, H-X. Liu, W. Chen, D-P. Huang, Dielectric evaluation of electrically tunable $\text{Ba}_{0.6}\text{Sr}_{0.4}\text{TiO}_3$ thick films prepared by screen printing, *Ceram. Int.* 38 (2012) 3465-3472.
- [7] A. Selmi, O. Khaldi, M. Mascot, F. Jomni, J.-C. Carru, Dielectric relaxations in $\text{Ba}_{0.85}\text{Sr}_{0.15}\text{TiO}_3$ thin films deposited on Pt/Ti/SiO₂/Si substrates by sol-gel method, *J. Mater. Sci.: Mater. Electron.* 27 (2016) 11299-11307.
- [8] Z. Yuan, J. Liu, J. Weaver, C.L. Chen, J.C. Jiang, B. Lin, V. Giurgiutiu, A. Bhalla, R.Y. Guo, Ferroelectric BaTiO_3 thin films on Ni metal tapes using NiO as buffer layer, *Appl. Phys. Lett.* 90 (2007) 202901.
- [9] Q. Xu, D. Zhan, D.P. Huang, H.X. Liu, W. Chen, F. Zhang, Effect of oxygen-ion motion on dielectric properties of $\text{Ba}_{0.6}\text{Sr}_{0.4}\text{TiO}_3$ thick films, *Materials Research Bulletin* 70 (2015) 99-105.
- [10] V. Walter, P. Delobelle, P.L. Moal, E. Joseph, M. Collet, A piezo-mechanical characterization of PZT thick films screen-printed on alumina substrate, *Sensors and Actuators A* 96 (2002) 157-166.
- [11] F. Xiang, H. Wang, M. Zhang, X. Sun, X. Yao, Preparation and dielectric tunability of bismuth-based pyrochlore dielectric thick films on alumina substrates, *Ceram. Int.* 34 (2008) 925-928.
- [12] **Y. Slimani, B. Unal, E. Hannachi, A. Selmi, M.A. Almessiere, M. Nawaz, A. Baykal, I. Ercan, M. Yildiz, Frequency and DC bias voltage dependent dielectric**

- properties and electrical conductivity of BaTiO₃-SrTiO₃/(SiO₂)_x nanocomposites, Ceram. Int. 45 (2019) 11989-12000.**
- [13] **C.G. Koops, On the dispersion of resistivity and dielectric constant of some semiconductors at audiofrequencies, Phys. Rev. 62 (1951) 121-124.**
- [14] A.K. Singh, Subrat K. Barik, R.N.P. Choudhary, P.K. Mahapatra, AC conductivity and relaxation mechanism in Ba_{0.9}Sr_{0.1}TiO₃, J. Alloys Compd. 479 (2009) 39-42.
- [15] S. Shannigrahi, F. Tey, K. Yao, R. Choudhary, Effect of Rare Earth (La, Nd, Sm, Eu, Gd, Dy, Er, Yb) Ion Substitution on the Microstructural and Electrical Properties of Sol-Gel Grown PZT Ceramics, J. Eur. Ceram. Soc. 24 (2004) 163-170.
- [16] **M.A. Almessiere, B. Unal, Y. Slimani, A. Demir Korkmaz, N.A. Algarou, A. Baykal, Electrical and dielectric properties of Nb³⁺ ions substituted Ba-hexaferrites, Results in Physics 14 (2019) 102468 (12 pages).**
- [17] **Y. Slimani, A. Selmi, E. Hannachi, M.A. Almessiere, M. Mumtaz, A. Baykal, I. Ercan, Study of tungsten oxide effect on the performance of BaTiO₃ ceramics, J. Mater. Sci.: Mater. Electron. 30 (2019) 13509-13518.**
- [18] A.K. Jonscher, The 'Universal' Dielectric Response, Nature 267 (1977) 673-679.
- [19] S. Mollah, K.K. Som, K. Bose, B.K. Chaudhuri, AC conductivity in Bi₄Sr₃Ca₃Cu_yO_x (y=0-5) and Bi₄Sr₃Ca_{3-z}Li_zCu₄O_x (z=0.1-1.0) semiconducting oxide glasses, J. Appl. Phys. 74 (1993) 931-937.
- [20] S.K. Barik, R.N.P. Choudhary, P.K. Mahapatra, Impedance spectroscopy study of Na_{0.5}Sm_{0.5}TiO₃ ceramic, Applied Physics A 88 (2007) 217-222.
- [21] A. Rouahi, A. Kahouli, A. Sylvestre, E. Defay, B. Yangui, Impedance spectroscopic and dielectric analysis of Ba_{0.7}Sr_{0.3}TiO₃ thin films, J. Alloys Compd. 529 (2012) 84-88.
- [22] **A. Khalfallaoui, L. Burgnies, K. Blary, G. Vélú, D. Lippens, J.C. Carru, Down scaling at submicron scale of the gap width of interdigitated Ba_{0.5}Sr_{0.5}TiO₃ capacitors, IEEE Trans. Ultrason. Ferroelect. Freq. Control 62 (2015) 247-254.**
- [23] C. Fu, C. Yang, H. Chen, L. Hu, Y. Wang, Ferroelectric properties of Ba_{0.6}Sr_{0.4}TiO₃ thin films with different grain sizes, Materials Letters 59 (2005) 330-333.
- [24] S.U. Adikary, H.L.W. Chan, Ferroelectric and dielectric properties of sol-gel derived Ba_xSr_{1-x}TiO₃ thin films, Thin Solid Films 424 (2003) 70-74.
- [25] P.Z. Ge, X.G. Tang, Q.X. Liu, Y.-P. Jiang, W.H. Li, B. Li, Temperature-dependent dielectric relaxation and high tunability of (Ba_{1-x}Sr_x)TiO₃ ceramics. J. Alloys Compd. 731 (2018) 70-77.

List of Figures

Figure 1.Preparation protocol of BST thick film capacitor structure

Figure 2.XRD patterns of BST thick film

Figure 3. SEM images of BST thick film.

Figure 4.Frequency dependence of (a) **the** dielectric **permittivity** and (b) **the** dielectric loss $\tan\delta$ of BST thick film for different temperatures

Figure 5. Temperature dependence of (a) the dielectric **permittivity** and (b) the dielectric loss measured at different frequencies.

Figure 6. Frequency dependence of the AC conductivity at various temperatures

Figure 7. (a) Capacitance- electric field (C-E) curve and (b) Polarization–Electric field (P-E) hysteresis **cycle**of BST thick film at room temperature.